

REGULARISED INTEGRAL EQUATIONS IN
CRACK SHAPE DETERMINATION PROBLEMS

(クラック形状決定問題に於ける正則化された積分方程式)

N. Nishimura (西村直志)

Dept. Civil Eng., Kyoto Univ.

1. Introduction

Let D be a bounded domain in R^2 which has a smooth boundary ∂D . Also let S be a smooth non-self-intersecting curve contained in D . The 2 dimensional (direct) crack problem for Laplace's equation is formulated into the following boundary value problem:

Find a function $u(\boldsymbol{x})$ in $D \setminus S$ which satisfies

$$\begin{aligned} \Delta u &= 0 \quad \text{in } D \setminus S, \\ \left(\frac{\partial u}{\partial n}\right)^+ &= \left(\frac{\partial u}{\partial n}\right)^- = 0 \quad \text{on } S, \\ \lim_{\boldsymbol{x}(\in S) \rightarrow \boldsymbol{x}_0(\in \partial S)} \varphi(\boldsymbol{x}) &= 0, \quad \varphi := u^+ - u^-, \end{aligned}$$

subject to a certain boundary condition (such as Dirichlet or Neumann conditions) on ∂D , where the superposed $+(-)$ indicates the limit on S from the positive (negative) side. In this statement, the positive (negative) side indicates the side of S into which (the negative of) the normal vector \boldsymbol{n} points.

The solution to this problem is well known to have an integral representation given by

$$u(\boldsymbol{x}) = \int_{\partial D} G(\boldsymbol{x} - \boldsymbol{y}) \frac{\partial u(\boldsymbol{y})}{\partial n} dS_y - \int_{\partial D} \frac{\partial G(\boldsymbol{x} - \boldsymbol{y})}{\partial n_y} u(\boldsymbol{y}) dS_y + \int_S \frac{\partial G(\boldsymbol{x} - \boldsymbol{y})}{\partial n_y} \varphi(\boldsymbol{y}) dS_y,$$

for $\boldsymbol{x} \in D \setminus S$, where $G(\boldsymbol{x} - \boldsymbol{y})$ is the fundamental solution of Laplace's equation given by

$$G(\boldsymbol{x} - \boldsymbol{y}) = -\frac{1}{2\pi} \log |\boldsymbol{x} - \boldsymbol{y}|.$$

The unknown halves of u and $\partial u/\partial n$ on ∂D and φ on S are determined from the boundary integral equations given by

$$\begin{aligned}
 0 &= -\frac{u(\mathbf{x})}{2} + \int_{\partial D} G(\mathbf{x} - \mathbf{y}) \frac{\partial u(\mathbf{y})}{\partial n} dS_y - \int_{\partial D} \frac{\partial G(\mathbf{x} - \mathbf{y})}{\partial n_y} u(\mathbf{y}) dS_y \\
 &\quad + \int_S \frac{\partial G(\mathbf{x} - \mathbf{y})}{\partial n_y} \varphi(\mathbf{y}) dS_y, \quad \mathbf{x} \in \partial D \\
 0 &= \frac{\partial}{\partial n_x} \left(\int_{\partial D} G(\mathbf{x} - \mathbf{y}) \frac{\partial u(\mathbf{y})}{\partial n} dS_y - \int_{\partial D} \frac{\partial G(\mathbf{x} - \mathbf{y})}{\partial n_y} u(\mathbf{y}) dS_y \right) \\
 &\quad + \int_S \frac{\partial}{\partial n_x} \frac{\partial}{\partial n_y} G(\mathbf{x} - \mathbf{y}) \varphi(\mathbf{y}) dS_y, \quad \mathbf{x} \in S
 \end{aligned} \tag{1a, b}$$

where the integration sign with a superimposed ∂ implies that the integral is carried out in the sense of Hadamard's finite part. The numerical method of solving crack problems with the help of discretised versions of these equations is called the double layer formulation of the boundary integral equation method (BIEM).

From a numerical point of view, the hypersingularity of the kernel function in (1b) has been the biggest difficulty associated with the otherwise attractive double layer potential formulation for crack problems. However, the so called regularisation techniques have reduced this difficulty considerably, and made this formulation a practical numerical tool of crack analysis. In particular, the stress function approach of regularisation proposed in [1] replaced all the nonintegrable kernel functions in this formulation by integrable ones. With this development, we are now ready to use BIEM in various practical crack problems.

The particular application considered in this paper is the inverse problem of determining the shape of a crack S from experimental data. Suppose that we somehow know that D contains one single crack S , whose shape and location, however, are unknown. We now try to determine S with the help of certain experiments. Namely, we prescribe a series of Dirichlet data u^I ($I = 1 \sim N$) on ∂D and measure the corresponding Neumann data $q^I := \partial u^I/\partial n$, or vice versa, where $N \geq 2$. In physical terms this corresponds to giving elastic antiplane displacements, electrostatic fields, etc. on ∂D and measuring the associated elastic traction, electric current, etc. We then reconstruct S in a manner

that these u^I 's and q^I 's are consistent with each other. This problem of crack shape determination from experiments has been investigated by Friedman & Vogelius[2]. They constructed two specific boundary data with which the uniqueness of the crack shape is conclusive. Kubo et al.[3] also discuss the same problem. In this paper, however, we shall be more interested in actually determining the shape of the crack with the help of the regularised boundary integral equations.

This paper begins with a new version of regularised integral equation for direct crack problems. This formulation allows the use of C^0 elements provided that the near tip behaviour of the solution be properly incorporated into the analysis. This is in contrast to the old version where one has to use C^1 elements. We then proceed to the inverse problem of crack shape determination. We shall determine S in a way that the L^2 norm of the RHS of (1a) is minimised subject to (1b). To this end we compute the variation of the Lagrangian functional associated with this minimisation problem to obtain a set of criteria of optimality. These criteria are nonlinear equations with respect to shape parameters of S , and are solved with the help of Newton's method. This process, however, requires derivatives of φ with respect to shape parameters. Bearing this in mind we derive hypersingular integral equations for these derivatives, which are also shown to allow the new version of regularisation. This paper concludes with a few numerical examples.

2. 'Integrated' regularised integral equations for direct crack problems

We shall consider a simplified version of (1b) given by

$$\oint_S n_i(\mathbf{x})n_j(\mathbf{y})G_{,ij}(\mathbf{x}-\mathbf{y})\varphi(\mathbf{y})dS_y = g(\mathbf{x}), \quad \mathbf{x} \in S \quad (2)$$

where g is a given function on S , and $\cdot_{,i}$ indicates the derivative with respect to the i th argument. We now notice that

$$G_{,ij}(\mathbf{x}) = -e_{ip}e_{jq}G_{,pq}(\mathbf{x}) \quad (3)$$

holds modulo Dirac's delta, where e_{ij} stands for the permutation symbol. Substitution

of (3) into (2) yields

$$-\frac{\partial}{\partial s_x} \int_S G(\mathbf{x} - \mathbf{y}) \frac{\partial \varphi}{\partial s}(\mathbf{y}) dS_y = g(\mathbf{x}), \quad (4)$$

from which one obtains a variational equation given by

$$\int_S \frac{\partial \psi}{\partial s}(\mathbf{x}) \int_S G(\mathbf{x} - \mathbf{y}) \frac{\partial \varphi}{\partial s}(\mathbf{y}) dS_y dS_x = \int_S \psi(\mathbf{x}) g(\mathbf{x}) dS_x, \quad (5)$$

where ψ is a test function bounded near ∂S , and s is the arc parameter of S which increases as one traces the crack viewing the positive side of S to the left. Furthermore, we set $s = 0$ at the mid-point of the crack and $s = \pm a$ at tips, where $2a$ is the arc length of S . Nédélec[4] proposed a Galerkin approach based on (5).

This variational formulation is more versatile than the collocation method proposed in [1] in that the former works with C^0 elements while the latter requires C^1 elements. Even with this property, however, this variational formulation may not be very practical because the double integration in (5) makes this method time consuming. An alternative to (5) which is devoid of this inefficiency is obtained by taking ψ to be piecewise constant:

$$\int_S (G(\mathbf{x}_1 - \mathbf{y}) - G(\mathbf{x}_0 - \mathbf{y})) \frac{\partial \varphi}{\partial s}(\mathbf{y}) dS_y = - \int_{x_0}^{x_1} g(\mathbf{x}) dS, \quad (6)$$

where $\mathbf{x}_0, \mathbf{x}_1$ are arbitrary points on S . In practice one takes sufficient number of pairs $(\mathbf{x}_0, \mathbf{x}_1)$ on S and computes (6) to get a system of linear equations for the discretised unknown φ . Some of the advantages of this formulation are (a) One may at least formally use C^0 shape functions. (b) The computational efficiency is not inferior to collocation. Actually, our experience shows that this method works well as long as the near tip behaviour of the solution is properly incorporated into the analysis.

3. Criteria of optimality in crack shape determination problems

We now proceed to the inverse problem of determining S from experimental data. As stated in **Introduction** we assume that the shape of S is unknown, but N pairs of both Dirichlet and Neumann data $u^I, q^I := \partial u^I / \partial n$ ($I = 1 \sim N$) on ∂D are known via some experimental means. We shall now determine S as the minimiser of

$$\sum_{I=1}^N \int_{\partial D} \left(f^I(\mathbf{x}) + \int_S G_{,i}(\mathbf{x} - \mathbf{y}) n_i(\mathbf{y}) \varphi^I(\mathbf{y}) dS_y \right)^2 dS_x \quad (7)$$

under the constrains of

$$g_{,i}^I(\mathbf{x})n_i(\mathbf{x}) + \oint_S n_i(\mathbf{x})n_j(\mathbf{y})G_{,ij}(\mathbf{x}-\mathbf{y})\varphi^I(\mathbf{y})dS_y = 0 \quad \text{on } S, \quad I = 1 \sim N \quad (8)$$

where (See (1).)

$$f^I(\mathbf{x}) = \frac{u(\mathbf{x})}{2} + \int_{\partial D} \frac{\partial G(\mathbf{x}-\mathbf{y})}{\partial n_y} u^I(\mathbf{y})dS_y - \int_{\partial D} G(\mathbf{x}-\mathbf{y})q^I(\mathbf{y})dS_y \quad \text{on } \partial D,$$

$$g^I(\mathbf{x}) = \int_{\partial D} \frac{\partial G(\mathbf{x}-\mathbf{y})}{\partial n_y} u^I(\mathbf{y})dS_y - \int_{\partial D} G(\mathbf{x}-\mathbf{y})q^I(\mathbf{y})dS_y \quad \text{on } S.$$

The use of the Lagrangian multiplier converts this problem into another of finding a stationary point of the following functional:

$$L := \frac{1}{2} \sum_{I=1}^N \int_{\partial D} \left(f^I(\mathbf{x}) + \int_S G_{,i}(\mathbf{x}-\mathbf{y})n_i(\mathbf{y})\varphi^I(\mathbf{y})dS_y \right)^2 dS_x$$

$$+ \sum_{I=1}^N \int_S \lambda^I(\mathbf{x}) \left(g_{,i}^I(\mathbf{x})n_i(\mathbf{x}) + \oint_S n_i(\mathbf{x})n_j(\mathbf{y})G_{,ij}(\mathbf{x}-\mathbf{y})\varphi^I(\mathbf{y})dS_y \right) dS_x, \quad (9)$$

where λ^I is the Lagrangian multiplier corresponding to (8). The function λ^I is assumed to be bounded near ∂S so that the integrals in the second term in (9) are convergent.

We next compute the variation of L . To facilitate this calculation we assume that S is at the optimal location S_0 , and take the coordinate in this configuration as the 'Lagrangian coordinate' \mathbf{X} . A varied configuration is then expressed in terms of a smooth one parametered mapping $\mathbf{x} = \mathbf{x}(\mathbf{X}, t)$ from $D \times [0, \epsilon[$ to D such that

$$\mathbf{x}(\mathbf{X}, \cdot) \text{ is one to one in } D, \quad \mathbf{X} = \mathbf{x}(\mathbf{X}, \forall t) \text{ for } \mathbf{X} \in \partial D, \quad \mathbf{x}(\mathbf{X}, 0) = \mathbf{X}, \mathbf{X} \in D \quad (10)$$

where $t \in [0, \epsilon[$ is a parameter and $\epsilon > 0$. Also, we define φ^I and λ^I to be functions of $\mathbf{X}(\in S_0)$ and t , whose values in a varied configuration are computed via $\varphi^I(\mathbf{x}^{-1}(\mathbf{x}, t), t)$, etc. L is then considered to be a functional of \mathbf{x} , φ^I and λ^I , which are functions of the 'Lagrangian coordinate' \mathbf{X} . Also the variation operator δ is now identical to $\partial/\partial t \cdot |_{t=0}$. These devices simplify the computation of the variations of L with respect to φ^I and λ^I . Actually, a standard variational calculus shows

$$\delta_{\lambda^I} L = 0 :$$

$$\oint_S n_i(\mathbf{x})n_j(\mathbf{y})G_{,ij}(\mathbf{x}-\mathbf{y})\varphi^I(\mathbf{y})dS_y = -n_i(\mathbf{x})g_i^I(\mathbf{x}), \quad \mathbf{x} \in S \quad (11)$$

$$\delta_{\varphi^I} L = 0 :$$

$$\oint_S n_i(\mathbf{x})n_j(\mathbf{y})G_{,ij}(\mathbf{x}-\mathbf{y})\lambda^I(\mathbf{y})dS_y = n_i(\mathbf{x})F_i^I(\mathbf{x}), \quad \mathbf{x} \in S \quad (12)$$

where

$$F^I(\mathbf{x}) := \int_{\partial D} G(\mathbf{x}-\mathbf{y}) \left(f^I(\mathbf{x}) + \int_S G_{,k}(\mathbf{y}-\mathbf{z})n_k(\mathbf{z})\varphi^I(\mathbf{z})dS_z \right) dS_y.$$

Notice that the RHSs of (11) and (12) are smooth functions on \bar{S} . This observation, together with the assumptions on the behaviour of φ^I and λ^I , shows that these functions have the following estimates near the tips:

$$\varphi^I \sim 4 \text{Sif}[\varphi^I]r^{1/2} + O(r^{3/2}), \quad \lambda^I \sim 4 \text{Sif}[\lambda^I]r^{1/2} + O(r^{3/2}), \quad r := |s \pm a|, \quad (13)$$

where $\text{Sif}[\cdot]$ indicates a number called ‘stress intensity factor’.

The variation of L with respect to \mathbf{x} is also computed in a standard manner, except that one has to pay attention to the hypersingularity of kernels. To illustrate this we compute

$$\delta_{\mathbf{x}} J, \quad J := \int_S \lambda(\mathbf{x}) \left(\oint_S n_i(\mathbf{x})n_j(\mathbf{y})G_{,ij}(\mathbf{x}-\mathbf{y})\varphi(\mathbf{y})dS_y \right) dS_{\mathbf{x}}, \quad (14)$$

where the superposed I in λ^I etc. has been suppressed for the purpose of simplicity. We first rewrite the integral in (14) by using the ‘regularisation’ in (4) and an integration by parts, followed by a change of variables to the Lagrangian coordinate. This process yields

$$J = \int_{s_0} \frac{\partial \lambda(\mathbf{x})}{\partial s_0} \int_{s_0} G(\mathbf{x}-\mathbf{y}) \frac{\partial \varphi(\mathbf{y})}{\partial s_0} dS_Y dS_X$$

where \mathbf{x} and \mathbf{y} are short for $\mathbf{x}(\mathbf{X}, t)$ and $\mathbf{x}(\mathbf{Y}, t)$. This expression depends on $\mathbf{x}(\mathbf{X}, t)$ only through the argument of G . Therefore the variation in question possesses the following expression:

$$\delta_{\mathbf{x}} J = \int_{s_0} \frac{\partial \lambda(\mathbf{x})}{\partial s_0} \int_{s_0} G_{,i}(\mathbf{x}-\mathbf{y})(\delta \mathbf{x}_i(\mathbf{x}) - \delta \mathbf{x}_i(\mathbf{y})) \frac{\partial \varphi(\mathbf{y})}{\partial s_0} dS_y dS_x \dagger \quad (15)$$

† From this formula onwards, we write \mathbf{x} etc. for \mathbf{X} etc., since they are identical at $t = 0$.

since the inner integrand is integrable for a smooth variation of S . For the purpose of the subsequent analysis, however, it is convenient to factor out the whole expression under the outer integration sign in (15) by $\delta \mathbf{x}$. Hence we split the inner integral in (15) into a sum of two singular integrals to obtain

$$\begin{aligned} \delta_{\mathbf{x}} J &= \int_{S_0} \delta \mathbf{x}_i(\mathbf{x}) \frac{\partial \lambda(\mathbf{x})}{\partial s_0} \int_{S_0} G_{,i}(\mathbf{x} - \mathbf{y}) \frac{\partial \varphi(\mathbf{y})}{\partial s_0} dS_y dS_x \\ &\quad - \int_{S_0} \frac{\partial \lambda(\mathbf{x})}{\partial s_0} \int_{S_0} G_{,i}(\mathbf{x} - \mathbf{y}) \delta \mathbf{x}_i(\mathbf{y}) \frac{\partial \varphi(\mathbf{y})}{\partial s_0} dS_y dS_x, \end{aligned} \quad (16)$$

where the integration sign with a superimposed $-$ indicates an integral in the sense of Cauchy's principal value. It is now obvious that we have to somehow change the order of integrations in the second term in (16). To this end, we prepare the following

Lemma. *Let $f(x, y)$ be a smooth function defined on $(x, y) = [-1, 1] \times [-1, 1]$. Then one has*

$$\begin{aligned} &\int_{-1}^1 \frac{1}{\sqrt{1-x}} \left(\int_{-1}^1 \frac{f(x, y)}{(x-y)\sqrt{1-y}} dy \right) dx \\ &= -\pi^2 f(1, 1) + \int_{-1}^1 \frac{1}{\sqrt{1-y}} \left(\int_{-1}^1 \frac{f(x, y)}{(x-y)\sqrt{1-x}} dx \right) dy. \end{aligned}$$

proof. A lengthy but straightforward calculation shows this result.

Corollary *Let φ and λ be functions which are defined on S and are smooth except at the tips ∂S , where they behave as in (13). Also let Ω be a smooth function on \bar{S} . Then one has*

$$\begin{aligned} &\int_S \frac{\partial \lambda(\mathbf{x})}{\partial s} \int_S \frac{\partial}{\partial s_y} G(\mathbf{x} - \mathbf{y}) \Omega(\mathbf{y}) \frac{\partial \varphi(\mathbf{y})}{\partial s} dS_y dS_x \\ &= -2\pi \left((\text{Sif}[\lambda] \text{Sif}[\varphi] \Omega)|_{\text{right tip}} - (\text{Sif}[\lambda] \text{Sif}[\varphi] \Omega)|_{\text{left tip}} \right) \\ &\quad + \int_S \frac{\partial \varphi(\mathbf{y})}{\partial s} \Omega(\mathbf{y}) \left(\frac{\partial}{\partial s_y} \int_S G(\mathbf{x} - \mathbf{y}) \frac{\partial \lambda(\mathbf{x})}{\partial s} dS_x \right) dS_y. \end{aligned}$$

With the last corollary it is now a simple matter to complete the calculation of $\delta_{\mathbf{x}} J$ in (14). Indeed one first decomposes the variation $\delta \mathbf{x}$ into its tangential and normal components to rewrite the second term in (16) into

$$- \int_{S_0} \frac{\partial \lambda(\mathbf{x})}{\partial s_0} \int_{S_0} G_{,i}(\mathbf{x} - \mathbf{y}) (t_i(\mathbf{y}) \delta \Omega(\mathbf{y}) + n_i(\mathbf{y}) \delta \omega(\mathbf{y})) \frac{\partial \varphi(\mathbf{y})}{\partial s_0} dS_y dS_x, \quad (17)$$

where t_i stands for the unit tangential vector to S directed into the positive direction of s , and $\delta\Omega$ and $\delta\omega$ are arbitrary functions defined on \bar{S} . Since $G_{,i}(\mathbf{x} - \mathbf{y})n_i(\mathbf{y})$ is integrable for a smooth S , one may interchange the two integrations in the 2nd term in (17). One then applies the foregoing corollary to the remaining term in (17), and returns to the 'Eulerian coordinate' to have

$$\begin{aligned} \delta_{\mathbf{x}}J = & \int_S \delta\omega(\mathbf{x}) \left(\frac{\partial\lambda(\mathbf{x})}{\partial s} \int_S n_i(\mathbf{x})G_{,i}(\mathbf{x} - \mathbf{y}) \frac{\partial\varphi(\mathbf{y})}{\partial s} dS_{\mathbf{y}} \right. \\ & \left. + \frac{\partial\varphi(\mathbf{x})}{\partial s} \int_S n_i(\mathbf{x})G_{,i}(\mathbf{x} - \mathbf{y}) \frac{\partial\lambda(\mathbf{y})}{\partial s} dS_{\mathbf{y}} \right) dS_{\mathbf{x}} \\ & + \int_S \delta\Omega(\mathbf{x}) \left(\frac{\partial\lambda(\mathbf{x})}{\partial s} \frac{\partial}{\partial s_{\mathbf{x}}} \int_S G(\mathbf{x} - \mathbf{y}) \frac{\partial\varphi(\mathbf{y})}{\partial s} dS_{\mathbf{y}} \right. \\ & \left. + \frac{\partial\varphi(\mathbf{x})}{\partial s} \frac{\partial}{\partial s_{\mathbf{x}}} \int_S G(\mathbf{x} - \mathbf{y}) \frac{\partial\lambda(\mathbf{y})}{\partial s} dS_{\mathbf{y}} \right) dS_{\mathbf{x}} \\ & - 2\pi \left((\text{Sif}[\lambda]\text{Sif}[\varphi]\delta\Omega)|_{\text{right tip}} - (\text{Sif}[\lambda]\text{Sif}[\varphi]\delta\Omega)|_{\text{left tip}} \right). \end{aligned} \quad (18)$$

This equation, (11) and (12) finally yield two more criteria of optimality for our problem in the following forms:

$$\begin{aligned} \delta_{\omega}L = 0 : \\ \sum_I \frac{\partial\lambda^I}{\partial s}(\mathbf{x}) \left(\frac{\partial g^I(\mathbf{x})}{\partial s} + \int_S n_i(\mathbf{x})G_{,i}(\mathbf{x} - \mathbf{y}) \frac{\partial\varphi^I}{\partial s}(\mathbf{y}) dS \right) \\ = \sum_I \frac{\partial\varphi^I(\mathbf{x})}{\partial s} \left(\frac{\partial F^I(\mathbf{x})}{\partial s} - \int_S n_i(\mathbf{x})G_{,i}(\mathbf{x} - \mathbf{y}) \frac{\partial\lambda^I}{\partial s}(\mathbf{y}) dS \right), \quad \mathbf{x} \in S \end{aligned} \quad (19)$$

$$\delta_{\Omega}L = 0 : \\ \sum_I \text{Sif}[\varphi^I](\mathbf{x})\text{Sif}[\lambda^I](\mathbf{x}) = 0. \quad \mathbf{x} \in \partial S \quad (20)$$

We thus conclude that the criteria of optimality for the minimisation problem given in (7) and (8) are (11), (12), (19) and (20).

Notice that the assumption that S is a straight line segment simplifies (19) considerably since one then has

$$n_i(\mathbf{x})G_{,i}(\mathbf{x} - \mathbf{y}) = 0 \quad \text{for } \mathbf{x}, \mathbf{y} \in S.$$

Indeed, this observation, together with the restriction that $\delta\omega, \delta\Omega$ are linear with respect

to s , reduces (19) into

$$\sum_I \int_S \omega^\alpha \left(\frac{\partial \lambda^I}{\partial s} \frac{\partial g^I}{\partial s} - \frac{\partial \varphi^I}{\partial s} \frac{\partial F^I}{\partial s} \right) dS, \quad (21)$$

where $\alpha = 1, 2$ and

$$\omega^1(\mathbf{x}) = \frac{a+s}{2a}, \quad \omega^2(\mathbf{x}) = \frac{a-s}{2a}.$$

Equations (11), (12) and (20), however, remain unchanged with this assumption.

One may now determine the shape of S by using these criteria and Newton's method as shown in the following steps:

- (1) Carry out more than 2 experiments to obtain u^I and q^I on ∂D . These data determine f^I and g^I in D for $I = 1 \sim N$.
- (2) Assume an initial shape for S . This initial shape has to be chosen close to the exact one for the present scheme to converge.
- (3) Solve (11) and (12) in this order for φ^I and λ^I ($I = 1 \sim N$). To this end, use the 'regularisation' of the type shown in (6).
- (4) See if (19) and (20) are satisfied to within an allowable error. If yes, one terminates the analysis. Otherwise one uses Newton's method to update the shape of S , and returns to the 3rd step.

Obviously one has to compute the derivatives of φ^I and λ^I with respect to shape parameters of S in the 4th step of the above scheme. The next section will be devoted to a method of computing these derivatives.

4. Regularised integral equations for derivatives with respect to shape parameters for S

As mentioned in the last section the determination of S by Newton's method requires derivatives of φ^I , λ^I , (19) and (20) with respect to shape parameters of S . This section discusses how one computes these derivatives. We shall henceforth denote these derivatives by $\dot{}$, which is essentially identical to δ in the last section.

To begin with, we consider $\dot{\varphi}^I$. One may expect that an integral equation for $\dot{\varphi}^I$ is obtained by taking the dot derivative of (11). This computation is made easier as one

introduces the Lagrangian coordinate and the mapping in (10). Indeed, a calculation similar to the one used in (18) proves

$$\begin{aligned} & \overline{\int_S n_i(\mathbf{x})n_i(\mathbf{y})G_{,ij}(\mathbf{x}-\mathbf{y})\varphi^I(\mathbf{y})dS_y} \\ &= -\frac{\partial}{\partial s_x} \int_S G_{,k}(\mathbf{x}-\mathbf{y})(\dot{x}_k(\mathbf{x})-\dot{x}_k(\mathbf{y}))\frac{\partial\varphi^I}{\partial s}(\mathbf{y})dS_y \\ & \quad + t_k(\mathbf{x})\frac{\partial\dot{x}_k}{\partial s}(\mathbf{x})\frac{\partial}{\partial s_x} \int_S G(\mathbf{x}-\mathbf{y})\frac{\partial\varphi^I}{\partial s}(\mathbf{y})dS_y - \frac{\partial}{\partial s_x} \int_S G(\mathbf{x}-\mathbf{y})\frac{\partial\dot{\varphi}^I}{\partial s}(\mathbf{y})dS_y. \end{aligned}$$

This result, (11) and $\Delta g^I = 0$ then give

$$\begin{aligned} \frac{\partial}{\partial s_x} \left[e_{ij}g_{,i}^I(\mathbf{x})\dot{x}_j(\mathbf{x}) + \int_S G_{,k}(\mathbf{x}-\mathbf{y})(\dot{x}_k(\mathbf{x})-\dot{x}_k(\mathbf{y}))\frac{\partial\varphi^I}{\partial s}(\mathbf{y})dS_y \right. \\ \left. + \int_S G(\mathbf{x}-\mathbf{y})\frac{\partial\dot{\varphi}^I}{\partial s}(\mathbf{y})dS_y \right] = 0, \end{aligned}$$

which permits an integration of the type given in (6) to yield

$$\begin{aligned} & \int_S G(\mathbf{x}_1-\mathbf{y})\frac{\partial\dot{\varphi}^I}{\partial s}(\mathbf{y})dS + e_{ij}g_{,i}^I(\mathbf{x}_1)\dot{x}_j(\mathbf{x}_1) \\ & \quad + \int_S G_{,k}(\mathbf{x}_1-\mathbf{y})(\dot{x}_k(\mathbf{x}_1)-\dot{x}_k(\mathbf{y}))\frac{\partial\varphi^I}{\partial s}(\mathbf{y})dS \\ &= \int_S G(\mathbf{x}_0-\mathbf{y})\frac{\partial\dot{\varphi}^I}{\partial s}(\mathbf{y})dS + e_{ij}g_{,i}^I(\mathbf{x}_0)\dot{x}_j(\mathbf{x}_0) \\ & \quad + \int_S G_{,k}(\mathbf{x}_0-\mathbf{y})(\dot{x}_k(\mathbf{x}_0)-\dot{x}_k(\mathbf{y}))\frac{\partial\varphi^I}{\partial s}(\mathbf{y})dS. \quad \mathbf{x}_0, \mathbf{x}_1 \in S \end{aligned} \tag{22}$$

Similarly one obtains an integral relation for $\dot{\lambda}^I$ given by

$$\begin{aligned} & \int_S G(\mathbf{x}_1-\mathbf{y})\frac{\partial\dot{\lambda}^I}{\partial s}(\mathbf{y})dS - e_{ij}F_{,i}^I(\mathbf{x}_1)\dot{x}_j(\mathbf{x}_1) \\ & \quad + \int_S G_{,k}(\mathbf{x}_1-\mathbf{y})(\dot{x}_k(\mathbf{x}_1)-\dot{x}_k(\mathbf{y}))\frac{\partial\dot{\lambda}^I}{\partial s}(\mathbf{y})dS \\ &= \int_S G(\mathbf{x}_0-\mathbf{y})\frac{\partial\dot{\lambda}^I}{\partial s}(\mathbf{y})dS - e_{ij}F_{,i}^I(\mathbf{x}_0)\dot{x}_j(\mathbf{x}_0) \\ & \quad + \int_S G_{,k}(\mathbf{x}_0-\mathbf{y})(\dot{x}_k(\mathbf{x}_0)-\dot{x}_k(\mathbf{y}))\frac{\partial\dot{\lambda}^I}{\partial s}(\mathbf{y})dS \\ & \quad - \int_{\mathbf{x}_0}^{\mathbf{x}_1} n_i(\mathbf{x}) \left(\int_{\partial D} G_{,i}(\mathbf{x}-\mathbf{y})E^I(\mathbf{y})dS_y \right) dS_x, \end{aligned} \tag{23}$$

where

$$E^I(\mathbf{x}) := e_{kl} \int_S G_{,k}(\mathbf{x}-\mathbf{y})\dot{x}_l(\mathbf{y})\frac{\partial\varphi^I}{\partial s}(\mathbf{y})dS_y + \int_S G_{,k}(\mathbf{x}-\mathbf{y})n_k(\mathbf{y})\dot{\varphi}^I(\mathbf{y})dS_y. \quad \mathbf{x} \in \partial D$$

With the solutions of (22) and (23), and formulae such as

$$\frac{\dot{\partial\varphi}}{\partial s} = \frac{\partial\dot{\varphi}}{\partial s} - \frac{\partial\varphi}{\partial s} \frac{\partial\dot{x}_i}{\partial s} t_i, \quad \overline{\text{Sif}[\dot{\varphi}]} = \text{Sif}[\dot{\varphi}] - \frac{1}{2} \text{Sif}[\varphi] \frac{\partial\dot{x}_i}{\partial s} t_i$$

one computes the dot derivatives of (19) and (20). One then utilises these derivatives in Newton's method for determining S . The expressions of these derivatives, however, are omitted because they are neither compact nor are they very difficult to obtain.

Finally, we notice that the terms of the form

$$\int_S G_{,k}(\mathbf{x} - \mathbf{y})(\dot{x}_k(\mathbf{x}) - \dot{x}_k(\mathbf{y})) \frac{\partial\varphi^I}{\partial s}(\mathbf{y}) dS_y \quad \mathbf{x} \in S$$

in (22) and (23) vanish when S is a straight line.

5. Numerical analysis

In this section we shall make several comments on the numerical techniques employed for obtaining the results to be given in the next section. Our main concern here is to describe precisely how we got our numerical solutions, rather than to recommend particular techniques. Hence the reader should bear in mind that the method to be discussed may not necessarily be useful in applications other than the present one.

(1) The 'integrated' regularised integral equations of the form in (6) are solved as follows:

1. Take nodal points \mathbf{x}^i ($i = 0 \sim n + 1$) on S in a way that \mathbf{x}^0 and \mathbf{x}^{n+1} coincide with the left and right tips, respectively.
2. Introduce a new variable τ defined by $s = a \sin(\pi\tau/2)$, and discretise φ^I etc. by using cubic spline functions in τ associated with the nodal points introduced in 1. This change of variable takes care of the near tip singularities of φ^I etc.
3. Write $n + 1$ equations obtained from (6) by setting

$$\mathbf{x}_1 = \mathbf{x}^i, \quad \mathbf{x}_0 = \mathbf{x}^{i-1}, \quad i = 1 \sim n + 1$$

consecutively.

4. Solve the resultant linear equations for n unknowns by using a least square solver.

(2) We found, by way of numerical experiments, that reduced degrees of freedom for the shape of S help to enhance the robustness of the crack shape determination analysis. We therefore assume that S is a straight line segment in the early stage of iterations. Namely we begin the analysis by using (11), (12), (21) and (20) to find a line segment located as close as possible to the true shape of S . We shall henceforth call this process a line search. As the line search converges, we switch to another analysis which allows full degrees of freedom to the shape of S . This analysis will be called a full search.

(3) Even in the line search, the process of the crack shape determination analysis is not as robust as would be desirable. Some improvement is achieved, however, by alternating directions of search for S : we may for example modify the shape of S only in the normal (tangential) direction in the even (odd) steps of Newton's method.

(4) In the full search we take as the shape parameters for S the coordinates of all nodes \boldsymbol{x}^i ($i = 0 \sim n + 1$). We therefore need $2(n + 2)$ equations to determine these parameters completely. Equation (19) evaluated at \boldsymbol{x}^i ($i = 1 \sim n$) provides n equations, while the same equation with $\partial\varphi^I(\boldsymbol{x})/\partial s$ etc. replaced by $\text{Sif}[\varphi^I](\boldsymbol{x})$ etc. gives two more equations at tips. Also (20) yields two equations. Finally n more constraints given by

$$\frac{|\boldsymbol{x}^{i+1} - \boldsymbol{x}^i|}{|\boldsymbol{x}^i - \boldsymbol{x}^{i-1}|} \text{ remains unchanged } (i = 1 \sim n)$$

are considered, so that the inter-node spacing keeps the same proportion during the iteration. We thus have as many equations as the number of unknowns.

6. Numerical examples

In this section we present several numerical examples of the crack shape determination analysis based on the proposed method.

We consider a circular domain having a radius of $2l$. In place of experiments we *compute* boundary data on ∂D by using BIEM for assumed exact crack locations, prescribing

on ∂D 8 Dirichlet data given by

$$\operatorname{Re}, \operatorname{Im}(x_1 + ix_2)^m, \quad m = 1 \sim 4.$$

The exterior boundary ∂D is modelled by 24 piecewise linear boundary elements, and 9 DOF ($n = 9$ in the notation used in the last section) spline elements are used for the crack.

In the first example the exact crack shape is a straight line having a length of $2l$ located at the centre of the domain. Figure 1 shows the mode of convergence from the indicated initial location. The line search was used throughout the whole convergence process.

The exact crack shape for the second example is a segment of a parabola shown in Fig. 2. The line search from the indicated initial location converged to a line segment near the parabola as shown in Fig. 2. Subsequent full search then led to a convergence to the exact location as depicted in Fig. 3.

7. Concluding remarks

(1) The use of Newton's method in the proposed method of crack shape determination is partly responsible for the occasional divergence of the scheme when the assumed initial location is not sufficiently close to the exact one. In practice it might be safer to attempt at a 'preprocessing' by using more robust, but not necessarily efficient, non-linear programming techniques to find a good initial location. In some cases other experimental information such as the AE source location data might be helpful for the same purpose.

(2) The results of the crack shape determination analysis presented here extend almost automatically to elastostatics.

(3) For an accurate crack analysis using the 'integrated' regularised integral equations, it is essential to use shape functions capable of introducing the correct near-tip singularities of φ etc.

Acknowledgement

The author wishes to express his gratitude to Mr. H. Kamiya for his help in the numerical work.

References

- [1] Nishimura, N. and Kobayashi, S., A regularized boundary integral equation method for elastodynamic crack problems, *Comp. Mech.*, 4, 319-328, 1989.
- [2] Friedman, A. and Vogelius, M., Determining cracks by boundary measurements, IMA preprint series #476, 1989.
- [3] Kubo, S., Sakagami, T. and Ohji, K., On the uniqueness of the inverse problem of identifying a crack by electric potential CT method, *Bull. JSME*, 59, 1989 (in Japanese).
- [4] Nédélec, J.C., Formulations variationnelles de quelques équations intégrales faisant intervenir des parties finies, *Innovative Numerical Analysis for the Applied Engineering Sciences* (Eds. R. Shaw et. al), Univ. Press of Virginia, 517-524, 1980.

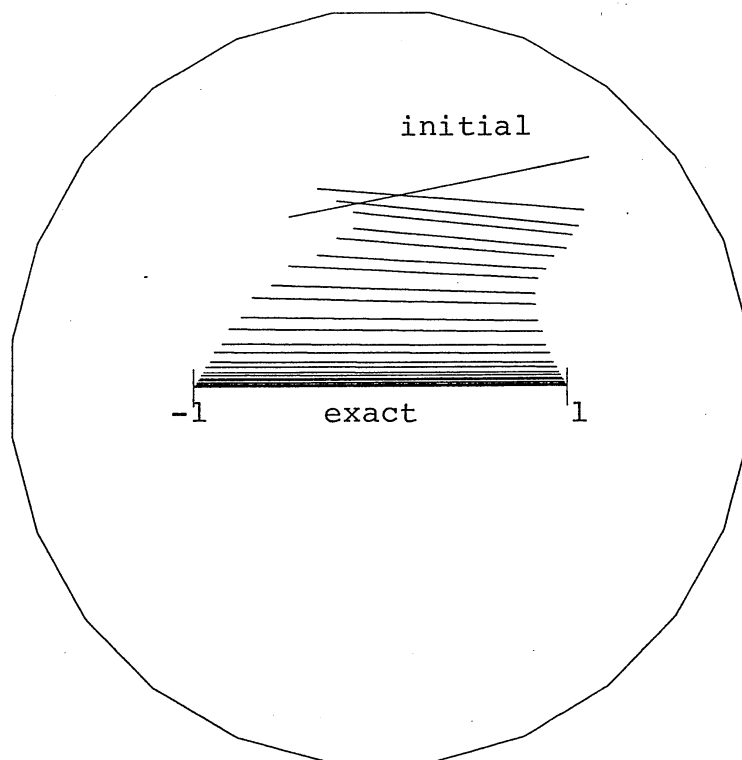


Fig. 1: Mode of convergence for a line crack

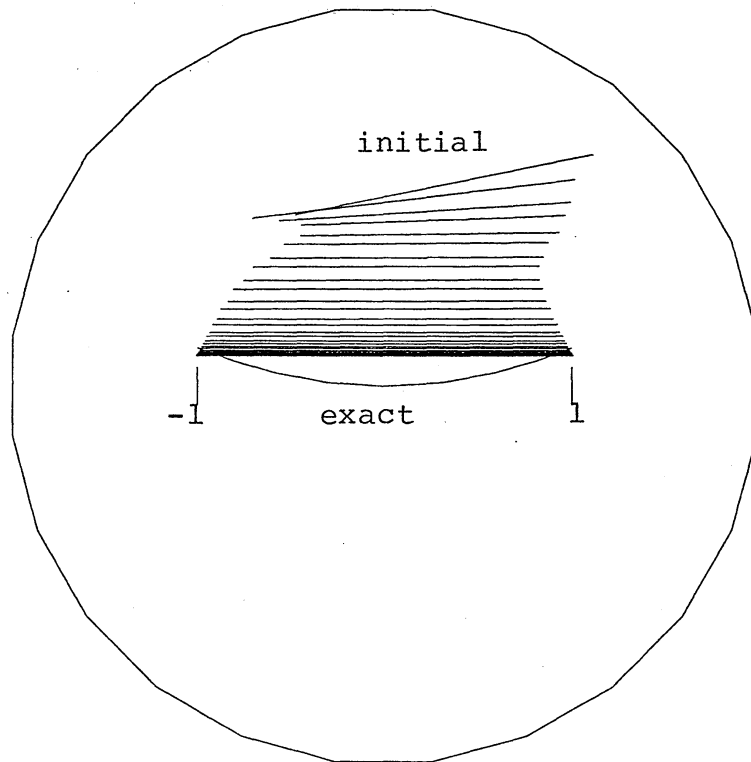


Fig. 2: Line search for a parabolic crack

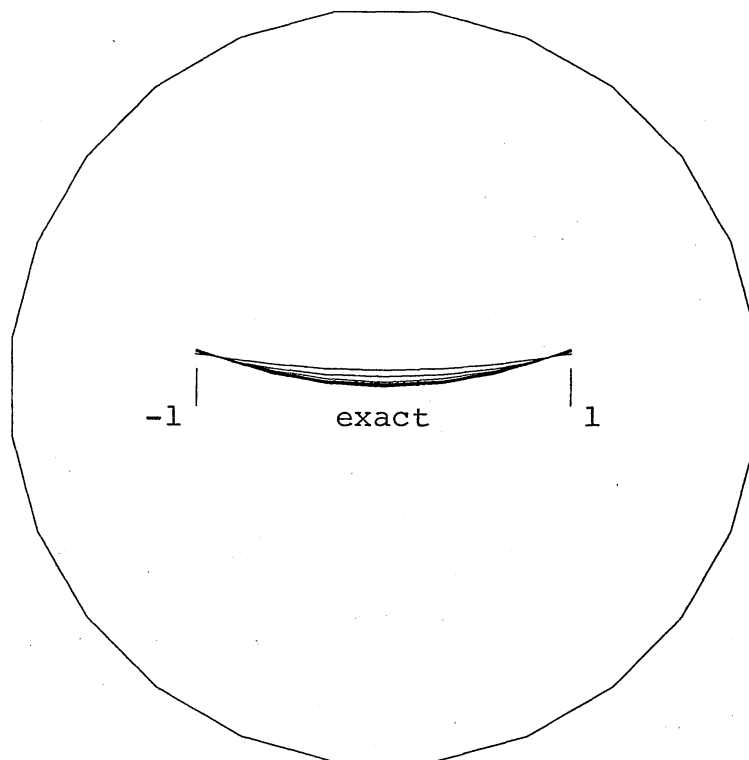


Fig. 3: Full search for a parabolic crack